The American Journal of Pathology, Vol. 184, No. 6, June 2014

ELSEVIER

The American Journal of
PATHOLOGY
ajp.amjpathol.org

VASCULAR BIOLOGY, ATHEROSCLEROSIS, AND ENDOTHELIUM BIOLOGY

# Inducing a Visceral Organ to Protect a Peripheral Capillary Bed

## *Stabilizing Hepatic HIF-1α Prevents Oxygen-Induced Retinopathy*

George Hoppe,* Tamara J. Lee,* Suzy Yoon,* Minzhong Yu,* Neal S. Peachey,*† Mary Rayborn,* M. Julieta Zutel,* George Trichonas,* John Au,* and Jonathan E. Sears*‡

*From the Cole Eye Institute,* Cleveland Clinic, Cleveland; the Louis Stokes Cleveland Veterans Affairs Medical Center,† Cleveland; and the Department of Cellular and Molecular Medicine,‡ Lerner Research Institute, Cleveland Clinic Lerner College of Medicine, Case Western Reserve University, Cleveland, Ohio*

Accepted for publication February 25, 2014.

Address correspondence to Jonathan E. Sears, M.D., Cleveland Clinic, Desk i-32, 9500 Euclid Ave., Cleveland, OH 44195. E-mail: searsj@ccf.org.

Activation of hypoxia-inducible factor (HIF) can prevent oxygen-induced retinopathy in rodents. Here we demonstrate that dimethyloxaloylglycine (DMOG)-induced retinovascular protection is dependent on hepatic HIF-1 because mice deficient in liver-specific HIF-1α experience hyperoxia-induced damage even with DMOG treatment, whereas DMOG-treated wild-type mice have 50% less avascular retina ($P < 0.0001$). Hepatic HIF stabilization protects retinal function because DMOG normalizes the b-wave on electroretinography in wild-type mice. The localization of DMOG action to the liver is further supported by evidence that i) mRNA and protein erythropoietin levels within liver and serum increased in DMOG-treated wild-type animals but are reduced by 60% in liver-specific HIF-1α knockout mice treated with DMOG, ii) triple-positive (Sca1/cKit/VEGFR2), bone-marrow–derived endothelial precursor cells increased twofold in DMOG-treated wild-type mice ($P < 0.001$) but are unchanged in hepatic HIF-1α knockout mice in response to DMOG, and iii) hepatic luminescence in the luciferase oxygen-dependent degradation domain mouse was induced by subcutaneous and intraperitoneal DMOG. These findings uncover a novel endocrine mechanism for retinovascular protection. Activating HIF in visceral organs such as the liver may be a simple strategy to protect capillary beds in the retina and in other peripheral tissues. *(Am J Pathol 2014, 184: 1890–1899; http://dx.doi.org/10.1016/j.ajpath.2014.02.017)*

Retinopathy of prematurity (ROP) is a potentially blinding disease that affects premature infants.[1] The disease is characterized by pathological angiogenesis and increased vasopermeability that lead to inoperable retinal detachment. ROP is likely responsible for the loss of eyesight in close to 10% of the approximately 1.5 million blind children worldwide, and as third-world countries improve their ability to keep premature infants alive, this number has the potential to increase.[2] The fetus develops in relative hypoxia *in utero*, a physiological state that is disrupted by premature birth and exacerbated by supplemental oxygen.[3] The presence of excess oxygen, which corresponds to the hyperoxic phase I of ROP, causes the regulatory enzyme prolyl hydroxylase domain protein (PHD) to hydroxylate two key proline residues within the oxygen-dependent degradation (ODD) domain of the hypoxia-inducible factor (HIF)-1α subunit, allowing it to become a substrate of the Von Hippel-Lindau protein, which targets the α subunit of HIF for degradation by the ubiquitin-proteasome pathway.[4–7] PHDs are a family of conserved enzymes with at least three

Supported by training grants from Fight For Sight (T.J.L.), Prevent Blindness Ohio (T.J.L.), The Hartwell Foundation (J.E.S.), the E. Matilda Zeigler Foundation (J.E.S.), the OneSight Foundation (J.E.S.), and a departmental grant from Research to Prevent Blindness.

G.H. and T.J.L. contributed equally to this work.

Disclosures: None declared.


http://dx.doi.org/10.1016/j.ajpath.2014.02.017

mammalian homologues (PHD1-3) that regulate HIF activity through post-translational modification and therefore quickly respond to hyperoxia.[8,9] Absence of HIF-1α results in halted downstream angiogenic pathways, including reduction of physiological vascular endothelial growth factor (VEGF) secretion early in postnatal, premature life that is associated with oxygen-induced vascular obliteration.[6,10–16]

Recent data from two randomized, prospective trials have defined the central paradox of oxygen therapy in severely premature infants: that oxygen is necessary to prevent mortality in these children but is simultaneously toxic to premature tissues such as the retina. The discovery of HIF proteins and their oxygen-dependent regulation through PHDs and Von Hippel-Lindau protein[17] offers a possible translational pathway for the growth and protection of blood vessels relevant to a broad range of diseases, including anemia,[18] stroke,[19,20] myocardial infarction,[21,22] skeletal muscle ischemia,[23] and ROP.[24–27]

Systemic injection of the HIF activator and nonselective inhibitor of HIF PHD, dimethyloxaloylglycine (DMOG), in phase I of oxygen-induced retinopathy (OIR), a rodent model of ROP, at postnatal days 6 and 8 (P6 and P8, respectively) resulted in a dramatic inhibition of OIR pathology that was recapitulated by systemic PHD2 ablation, and, to a definite but lesser extent, by systemic PHD1 ablation.[24–26] Surprisingly, hepatic HIF-1α protein levels after DMOG injection in mice were dramatically up-regulated compared with levels in brain, retina, and kidney. Organ lysate obtained from DMOG-treated mice expressing a transgene of luciferase fused to the ODD (luc-ODD)[28] demonstrated highest luciferase activity in the liver.[24] This unusual finding of liver-specific HIF-1α activation and subsequent protection of the retinal vasculature initiated the hypothesis that the liver could be stimulated to protect retinal capillary beds via hepatic PHD inhibition (PHDi). Here we show that the liver can be directly involved in the prevention of OIR as seen in the DMOG-treated mice.

## Materials and Methods

### OIR and Preparation of Retinal Flat Mounts

The murine model of ROP used in this study is based on a well-established protocol by Smith et al,[29] which involves exposing pups and their nursing mothers to 5 days of hyperoxia (75% oxygen) during P7 through P12 in the wild-type C57BL/6 (WT) pups. A Plexiglas incubator with an oxygen sensor and feedback system (ProOx, Biospherix, Ltd., Lacona, NY) was used to ensure continuous hyperoxia. Animals were injected with 200 μg/g DMOG i.p. or an equivalent volume of control phosphate-buffered saline (PBS) at P6, P8, and P10. After hyperoxia, the pups were returned to room-air (normoxic) conditions through P17, at which point they were studied. Flat mount preparation and lectin (GS-IB4-Alexa568, Life Technologies Corporation, Grand Island, NY) staining were performed essentially as described elsewhere.[30,31] Retinas were dissected using four radial cuts, and flat-mounted onto glass slides with Vectashield mounting medium (Vector Laboratories, Burlingame, CA). All animal procedures were performed in accordance with guidelines from the Cleveland Clinic Institutional Animal Care and Use Committee.

### Quantification of Retinal Flat Mounts

For quantitative analysis of avascular area, vascular tortuosity, and tufting, retinal images were batch-processed using a customized macro and algorithms generated in Image-Pro Plus version 7.0 (Media Cybernetics, Inc., Rockville, MD) as previously described.[24]

### Electroretinography

After overnight dark-adaptation, mice were anesthetized with 80 mg/kg ketamine and 16 mg/kg xylazine. Eye drops were used to dilate the pupil (1% tropicamide; 1.5% phenylephrine HCl), to anesthetize the corneal surface, and to make contact with the corneal recording electrode (1% methylcellulose). Dark-adapted electroretinograms (ERGs) were recorded to strobe-flash stimuli presented in a ganzfeld system (LKC Technologies, Inc., Gaithersburg, MD). ERGs were recorded using a thin, stainless steel wire that contacted the corneal surface. Needle electrodes were placed in the cheek and tail to serve as reference and ground leads. ERG signals were recorded using a UTAS E-3000 signal-averaging system (LKC Technologies, Inc).

### Generation and Confirmation of Genotype for HIF-1α Knockout Mice

Liver-specific HIF-1α knockout (KO) mice were generated at The Jackson Laboratory (Bar Harbor, ME) by crossing an *HIF1A 2-lox* strain with an albumin-Cre strain, both on C57BL/6 genetic backgrounds. Fusion of Cre-recombinase to the albumin promoter allows for loss of *HIF1A* in the majority (80%) of hepatocytes. To confirm the lack of the liver *HIF1A* gene in the HIF-1α KO mice, total DNA was extracted from murine liver, kidney, and retina samples by digesting overnight at 55°C in 200 μL of Direct PCR Lysis reagent (Viagen Biotech Inc., Los Angeles, CA) and 1 μL of proteinase K (Qiagen, Germantown, MD). PCR was performed in Taq PCR Master Mix (Promega Corporation, Madison, WI) at 94°C for 3 minutes, followed by 25 cycles of 30 seconds at 94°C, 60 seconds at 55°C, and 60 seconds at 72°C. The reaction was terminated at 72°C for 10 minutes. DNA ladder 1 Kb Plus (Life Technologies Corporation) was used as a standard in 4% agarose gel to determine PCR product sizes. The following primers were used to detect *2-lox* (recombined), *1-lox* (nonrecombined), and wild-type alleles: FwdI (5′-TTGGGGATGAAAACATCTGC-3′), FwdII (5′-GCAGTTAAGAGCACTAGTTG-3′), and Rev (5′-GGAGCTATCTCTCTAGACC-3′). The *HIF-1α 1-lox* allele was identified as a 270-bp band, the *2-lox* allele was identified

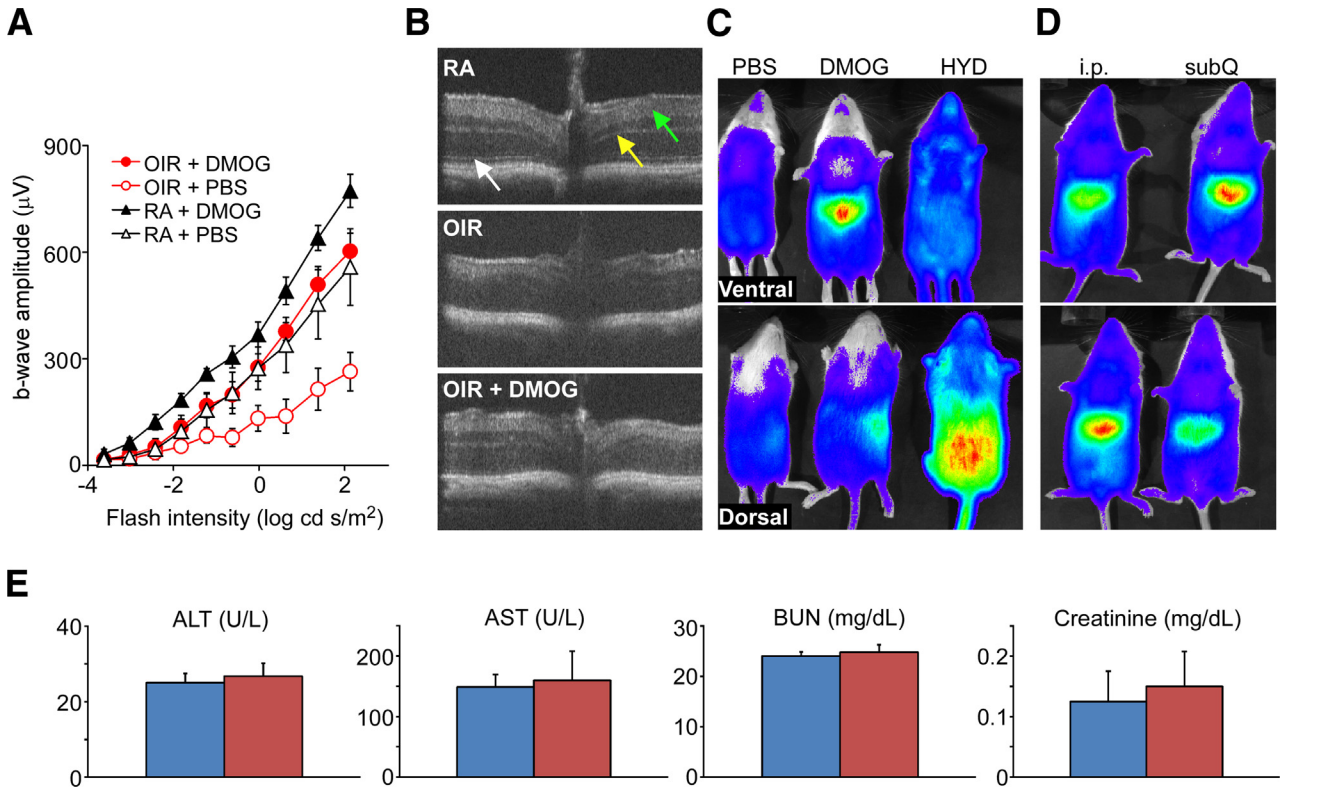


**Figure 1** Functional and structural outcomes of HIF PHDi. **A:** ERGs taken at P17 compare b-wave amplitude of four different groups of mice. Animals exposed to room air or the OIR cycle and treated with sham i.p. injection of PBS had the lowest deflection, indicating decreased function of the retina. Responses of OIR DMOG-injected mice were significantly higher in b-wave amplitude as compared to OIR PBS-injected mice ($P < 0.05$). Normoxic sham-injected and OIR DMOG-injected animals were equal in waveform amplitude, showing that HIF PHDi protected retinal function in hyperoxia/hypoxia, restoring it to levels of normoxic-raised pups. Normoxic DMOG-injected animals had supernormal deflection, demonstrating that DMOG improved retinal function in normoxia and therefore caused no degradation of retinal function. **B:** Spectral domain ocular coherence tomography noninvasively shows how DMOG protected retinal structure from OIR pathology. Note the high level of structural resolution in the **upper** and **lower panels**, which is lost from the **middle panel**, with attention to the photoreceptor inner/outer segment boundary, outer plexiform layer, and inner plexiform layer (**white**, **yellow**, and **green arrows**, respectively). **C:** Imaging of the luc-ODD mouse reveals the *in vivo* reporter genetic assessment of where DMOG had a molecular target. DMOG targets the liver, seen as on central luminescence in the ventral view and in the right lateral aspect of the dorsal view, whereas hydralazine (HYD), a known inhibitor of PHD and antihypertensive medicine, targets the kidneys, seen as lower symmetrical retroperitoneal hyperfluorescence in the dorsal view. PBS control shows no luminescence. **D:** DMOG targets liver for HIF stabilization regardless of the administration route, i.p. or subcutaneous (subQ); two independent experiments are shown in the **upper** and **lower panels**. **E:** Blood values of parameters that serve as indicators of liver or kidney toxicity following treatment with PBS (blue bars) or DMOG (red bars). Data are expressed as means ± SEM (**A** and **E**). $n = 3$ mice per group (**A** and **E**). ALT, alanine aminotransferase; AST, aspartate aminotransferase; BUN, blood urea nitrogen.

as a 260-bp band, and the wild-type (WT) allele was identified as a 240-bp band.[18]

## Histology

Tissue samples from WT and HIF-1α KO mice were harvested, rinsed briefly in PBS, and fixed overnight in 2% paraformaldehyde/2% glutaraldehyde. Diagonal liver sections, transverse kidney sections, and posterior coronal brain sections were obtained and embedded in paraffin. Tissues were stained using H&E. Additional histological analysis involved retina fixed in 4% PFA for paraffin-embedded sections and stained with toluidine blue. All histopathological changes were assessed by a pathologist using masked specimens, with attention to preservation of gross architecture, cellular structure, and vascularity, as well as any evidence of apoptotic or inflammatory changes.

## Western Blot Analysis

Mice were sacrificed by ketamine/xylazine overdose, and organs were collected and placed in radioimmunoprecipitation assay buffer (200 μL per 50 mg of tissue, pH 7.0) containing Complete Protease Inhibitors (Roche Diagnostics, Indianapolis, IN), disrupted using a tight-fitting microtube pestle, and centrifuged to remove particulate matter. A Pierce BCA protein assay kit (Thermo Fisher Scientific Inc., Rockford, IL) was used to measure protein concentrations. Lysates were subjected to 4% to 20% SDS-PAGE and electrotransferred to polyvinylidene difluoride membrane for immunoblotting. Membranes were blocked with 5% nonfat dried milk in

Tris-buffered saline and 0.1% Tween 20, then probed with anti–HIF-1α antibody (Cayman Chemical Company, Ann Arbor, MI) overnight. After washing and secondary antibody hybridization, membranes were exposed by chemiluminescence (Western Lightning, PerkinElmer Inc., Waltham, MA).

### Reverse Transcription and Quantitative PCR

Tissue from liver, kidney, brain, and retina was placed into 1 mL of RNAlater reagent (Qiagen) and stored at −80°C. Total RNA was extracted using RNeasy kit (Qiagen) and measured using NanoDrop (Thermo Fisher Scientific Inc.) and standard spectrophotometric parameters. RNA (1 μg) from each sample was retrotranscripted to cDNA using QuantiTect Reverse Transcription Kit (Qiagen). cDNA samples (1 mL) were used as template for amplification reactions performed with the QuantiTect SYBR Green PCR kit (Qiagen) following the manufacturer's instructions. PCR amplifications were performed in a 7900HT Fast Real-Time PCR system (Applied Biosystems, Foster City, CA) and quantitative PCR data analysis was performed with Re-Quantification Managed software version 2.2.2 (Applied Biosystems).

### *In Vivo* Localization of PHD Inhibition

The *Gt(ROSA)26Sor*$^{tm1(Luc)Kael}$ (luc-ODD) mice were obtained from The Jackson Laboratory. Pups were given i.p. injections of 200 μg/g DMOG 3 hours before live imaging. Mice were injected with a mixture of 100 mg/kg ketamine, 10 mg/kg xylazine, and 50 mg/kg luciferin and placed in a light-tight chamber connected to a supercooled charge-coupled camera. Photons were collected for 15 seconds using an IVI 100 Imaging System (PerkinElmer Inc.).

### Immunohistochemistry

WT and HIF-1α KO P8 pups were injected with 200 μg/g DMOG i.p. and sacrificed 3 hours later by lethal ketamine/xylazine injection. The median hepatic lobe was excised and immediately placed in 4% paraformaldehyde (PFA)in PBS. Livers were fixed for 3 days in PFA at 4°C, followed by paraffin embedding and preparation of 5 μm sections. Liver paraffin-embedded sections were deparaffinized in xylene and rehydrated in a battery of ethanol solution. Antigen retrieval was performed in a water bath at 99°C using Target Retrieval Solution (Dako North America, Inc., Carpinteria, CA). Immunohistochemistry was performed using anti–HIF-1α rabbit monoclonal antibody (clone EP1215Y, Millipore Corporation, Billerica, MA) and revealed using an anti-rabbit Vectastain Elite ABC peroxidase kit (avidin-biotin system) followed by an ImmPACT VIP peroxidase substrate kit (Vector Laboratories).

### Erythropoietin ELISA

Six hours after 200 μg/g DMOG i.p. injection, WT and HIF-1α KO P8 mouse pups were anesthetized by ketamine/xylazine and blood was drawn using a heparinized 27-gauge needle and syringe. Serum was diluted 1:10 with sample diluent provided by the manufacturer of murine erythropoietin (EPO) colorimetric enzyme-linked immunosorbent assay (ELISA; R&D Systems, Inc., Minneapolis, MN). Spectrophotometric measurements of EPO quantities were obtained according to the manufacturer's instructions.

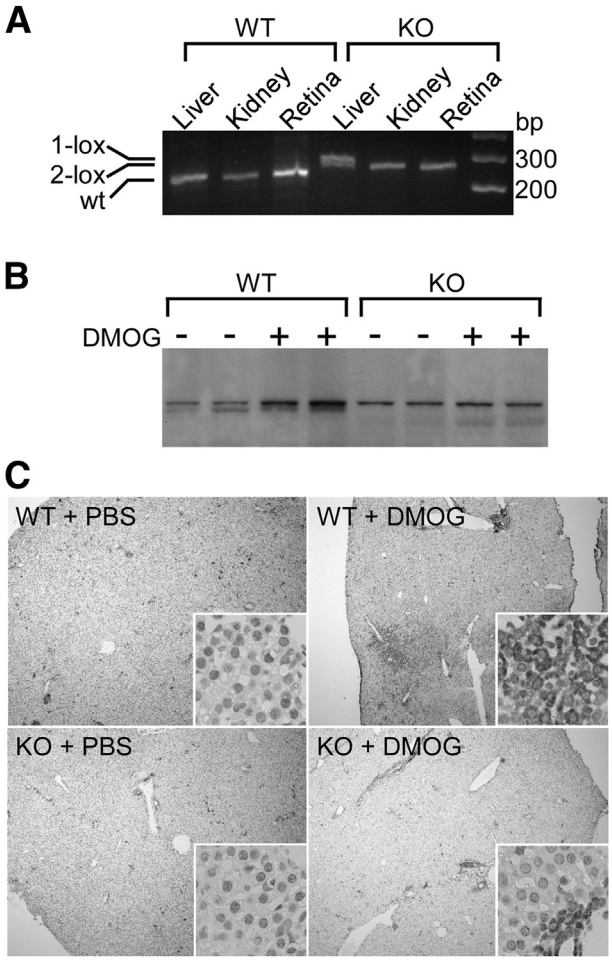


**Figure 2** Cre-lox recombination of liver-specific HIF-1α KO. **A:** Ablation is shown in liver compared to kidney and retina by PCR-amplified fragments of the recombination site within the *HIF1A* gene. *1-lox* and *2-lox* designate the recombined (270-bp) and nonrecombined (260-bp) alleles, respectively, and the WT allele (240 bp). **B:** Western blot analysis shows residual HIF-1α expression from liver-derived cells that do not express albumin, such as mesenchymal fibroblasts and endothelial, epithelial, stellate, and Kupffer cells. Only the WT had DMOG-inducible HIF-1α protein, whereas the HIF-1α KO expressed HIF-1α, but without effect from DMOG. **C:** Immunohistochemistry using HIF-1α antibody shows increased protein content in liver paraffin sections taken from DMOG- versus PBS-treated animals in WT only when compared to HIF-1α KO. Original magnification: ×40 (**C**), ×400 (**C**, **insets**).

### Flow Cytometry

Bone-marrow–derived endothelial precursor cell (EPC) response to DMOG was measured by isolation and quantification of leukocytes expressing triple-positivity for the

cell-surface receptors Sca-1, cKit, and VEGFR2. White blood cell isolates were obtained from peripheral blood and then tagged with Sca-1, cKit, and VEGFR2 fluorescent antibodies (BD Biosciences, San Jose, CA). Cells were then counted using an LSRII flow cytometer (BD Biosciences) calibrated before each experiment, and analyzed using FlowJo software version 10 (Tree Star Inc., Ashland, OR).

### Statistical Analysis

ERG measures were evaluated with a two-way repeated-measures analysis of variance. All other data were analyzed by comparing means using the Student *t*-test. The two-tailed probability associated with rejecting the null hypothesis of no difference between observed groups was calculated, using an $\alpha$ level of 0.05.

## Results

### Stabilization of HIF-1$\alpha$ via PHD Inhibition Prevents OIR in Mice and Targets Hepatic PHD

We previously reported quantitative analysis of retinal flat mounts in both mice and rats using both sustained and fluctuating oxygen protocols demonstrating that PHDi prevents oxygen-induced retinovascular growth attenuation and

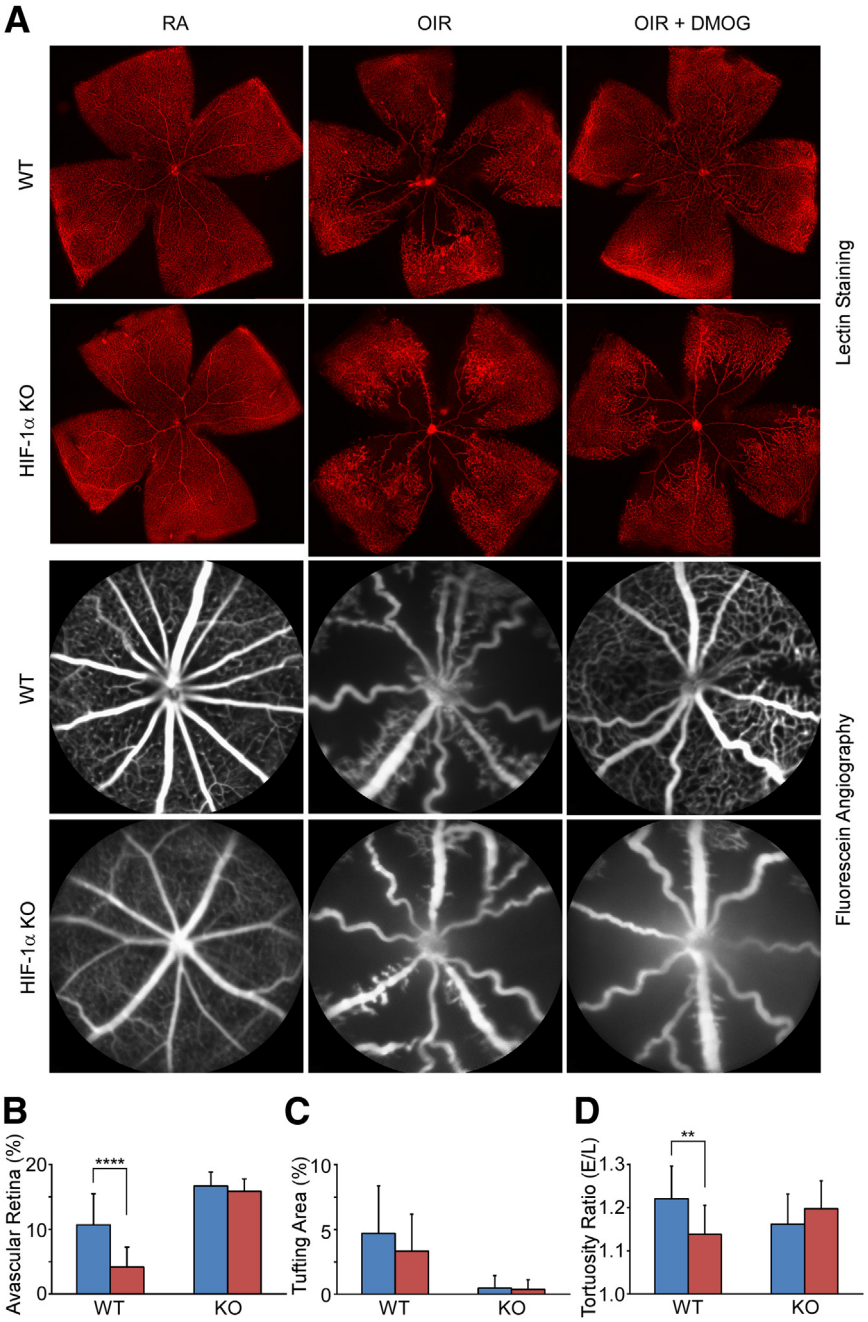


**Figure 3** The effect of hepatic *HIF1A* ablation on retinovascular protection by DMOG at P17. **A:** Lectin staining shows typical OIR pathology manifested as capillary dropout/avascularity that was prevented by i.p. DMOG injection, demonstrated here as robust preservation of central capillaries. In contrast, the liver HIF-1$\alpha$ KO mouse developed typical OIR pathology, characterized by capillary dropout seen surrounding the optic nerve, that was not prevented by DMOG, as it was in WT. *In vivo* fluorescein angiograms highlight posterior avascularity in the OIR model WT mouse that was prevented by HIF PHDi by DMOG. Fluorescein angiography confirms results from lectin-stained retinas shown above and demonstrates that DMOG could not prevent capillary loss in the HIF-1$\alpha$ KO mouse as it did in the WT mouse. Computerized quantification (see Sears et al[24] for details) of avascular retinal area (**B**); retinal area with neovascular tufts (**C**); and vascular tortuosity (**D**) confirm the failure of DMOG to prevent OIR-associated vascular pathology. PBS, blue bars; DMOG, red bars. Data are expressed as means $\pm$ SEM (**B-D**). $n = 20$ eyes per group (**B-D**). $^{**}P < 0.01$, $^{****}P < 0.0001$, *t*-test.

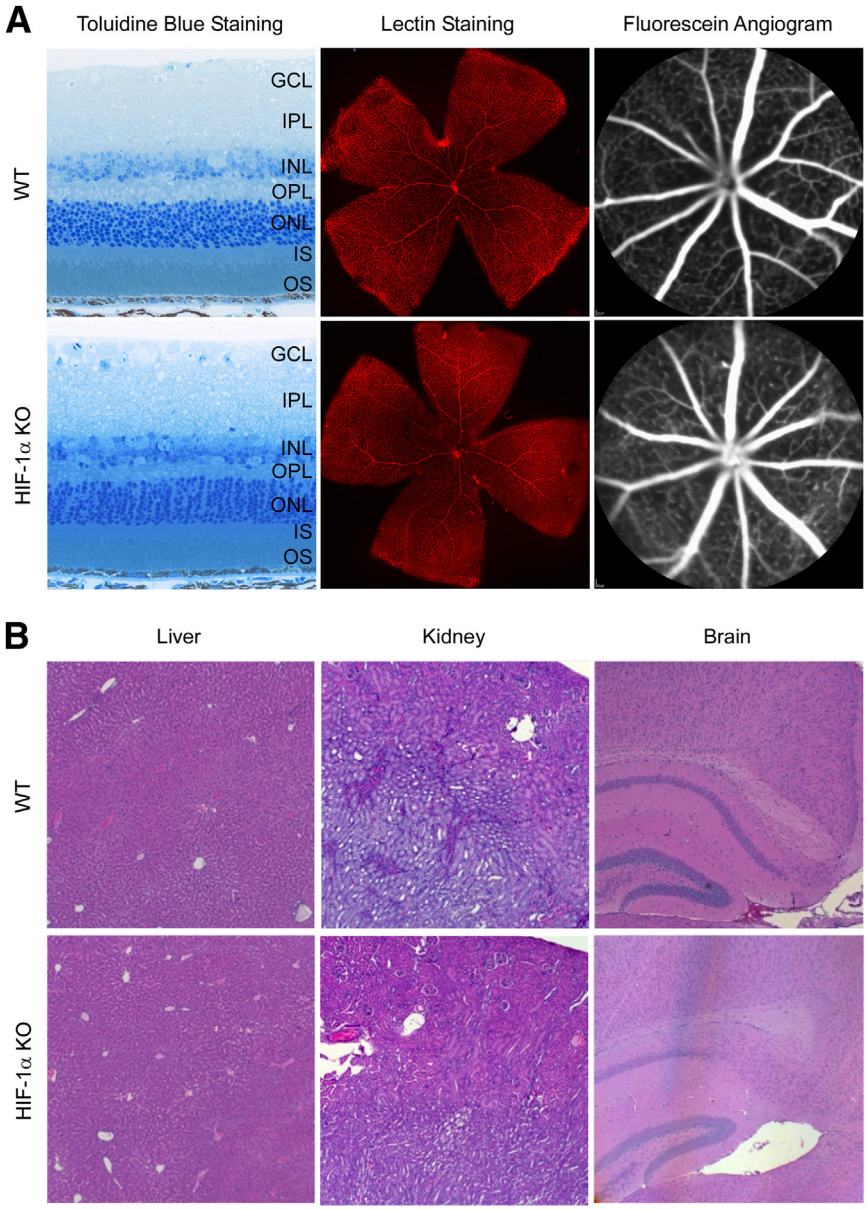


**Figure 4** HIF-1α KO mouse developed normal retina, liver, kidney, and brain. **A:** Toluidine blue staining, lectin staining, and *in vivo* fluorescein angiography show normal retinal histology and retinal blood vessels in WT mice. HIF-1α KO mouse had a similar phenotype as in WT. **B:** Gross microsections stained with H&E show a similar phenotype between normoxic WT and HIF-1α KO mice of liver, kidney, and brain. GCL, ganglion cell layer; INL, inner nuclear layer; IPL, inner plexiform layer; IS, inner segment; ONL, outer nuclear layer; OPL, outer plexiform layer; and OS, outer segment of photoreceptors.

vasoobliteration.[24,27] We now correlate the functional outcome of DMOG hypoxia mimetic treatment measured by ERG (Figure 1A).

The b-wave reduction observed in OIR animals without DMOG was prevented by DMOG treatment, and response amplitudes of DMOG-treated OIR animals were equivalent to those in mice reared in room air. This demonstrates that the strategy of HIF stabilization through PHDi preserves retinal function in animals subjected to the OIR cycle. WT normoxic pups also show higher b-wave amplitude in response to HIF PHDi that is not statistically significant at all flash intensities. We hypothesize that this supernormal trend may have been secondary to more robust oxygen delivery from HIF PHDi because of increased blood supply, the cytoprotective capability of HIF stabilization, or cytokines such as EPO that the liver secretes in response to systemic HIF PHDi. Although these are at this point hypotheses only, the trend does demonstrate that HIF PHDi is not toxic to normal retinal function. Spectral domain ocular coherence tomography, shown in Figure 1B, permits the collection of alternative, cross-sectional, in-depth views of specific regions of interest that are suggestive of ischemia, neovascularization, or edema. Spectral domain ocular coherence tomography revealed striking preservation of retinal cell layers when comparing normoxia to hyperoxia or hyperoxia with HIF PHDi (Figure 1B). *In vivo* whole-animal studies using the luc-ODD mouse[28] presented here (Figure 1, C and D) correlate with previously published organ lysate measurements and Western blots comparing time and dose response for retinal and hepatic HIF.[24] The luc-ODD mouse expresses a fusion protein

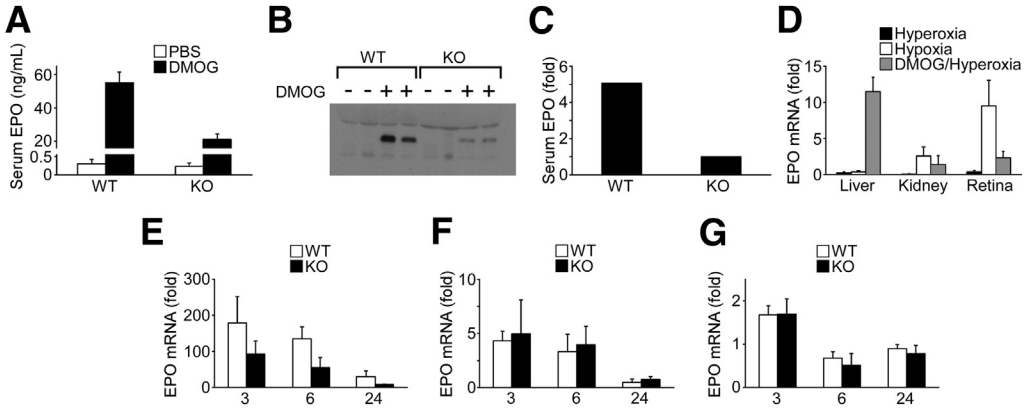


**Figure 5** Response to DMOG revealed an increase in liver and serum EPO levels in WT mice that was blunted in HIF-1α KO mice, in synchrony with mRNA measurements of DMOG-treated WT mice and HIF-1α KO mice. **A:** Pronounced up-regulation of serum EPO measured by ELISA was present in DMOG-injected WT mice 6 hours after DMOG injection; serum EPO was reduced by 60% in HIF-1α KO mice. **B:** Representative Western blot analysis of serum at 6 hours demonstrates increased EPO in WT murine serum and reduced levels of serum EPO in a HIF-1α KO mouse. The Western blot was repeated three times, with different samples obtained identically. **C:** Densitometry of the Western blot from **B**. **D:** Densitometry values were averaged from WT + DMOG and HIF-1α KO + DMOG. EPO mRNA from murine organs after 5 days of hyperoxia at P12 (Hyperoxia), or at the peak of hypoxic ischemia P17 (Hypoxia), or 24 hours after DMOG injection in hyperoxia (DMOG/Hyperoxia). Both the kidney and eye responded to hypoxia by increasing EPO synthesis, whereas the liver showed no response to hyperoxia/hypoxia. Yet, it is the liver alone that had a strong response to DMOG in hyperoxia. **E**–**G:** Analysis of mRNA from WT versus HIF-1α KO P8 mice at 3, 6, and 24 hours after DMOG injection. There was a notable increase in EPO mRNA in the liver of approximately 200-fold (**E**) as compared to that in the kidney (approximately 5-fold) (**F**) and that in the retina (approximately 2-fold) (**G**). The *y* axes represent fold-change from mRNA measurement at zero time point (0 hours). Data are expressed as means ± SEM (**A**, **D**–**G**). $n = 6$ mice per group (**A** and **D**); $n = 4$ mice per group (**E**–**G**).

transgene of luciferase and the ODD, thereby serving as an *in vivo* reporter gene construct to identify where HIF PHD is inactivated and HIF is stabilized. Whole-animal imaging 3 hours after DMOG injection generates a liver-specific luminescence pattern in contrast to hydralazine, a hydrazine with known PHDi activity or PBS (Figure 1C). DMOG induces luminescence in the liver, visualized in the upper abdomen, ventral side, and right lateral aspect, dorsal side, compared to hydralazine, which causes hyperluminescence in the kidneys, seen as most intense in the lower retroperitoneal space, dorsal side, whereas PBS, a negative control, produces no luminescence. In addition, subcutaneous injection of DMOG (Figure 1D) also causes hepatic luminescence, demonstrating that DMOG is active against HIF PHD in the liver by both intraperitoneal and subcutaneous delivery. Despite this liver tropism, DMOG-treated animals have normal liver and kidney function parameters after DMOG injection, demonstrating no toxicity when assessed by liver and kidney function blood tests (Figure 1E).

## Hepatic HIF-1α Is Required for DMOG-Mediated Prevention of OIR

Given preliminary work and the data shown in Figure 1, which suggests that systemic DMOG uniquely stabilizes hepatic HIF while protecting retinal blood vessels from hyperoxia, we speculated that liver-specific HIF might be integral to DMOG-mediated prevention of retinovascular pathology from hyperoxia. We thus generated a conditional cre/lox HIF-1α (*HIF1A*$^{2lox/2lox}$; albumin-Cre) hepatic knockout (HIF-1α KO) mouse to determine whether liver-specific HIF-1α is required for retinovascular protection by DMOG. Confirmation of hepatic *HIF1A* ablation was obtained via genotyping (Figure 2A), liver protein analysis (Figure 2B), and immunohistochemistry (Figure 2C). Note that there is constitutive expression of HIF-1α from hepatic cells that do not express albumin, for example, endothelial, stellate, or Kupffer cells, but there is no induced expression after DMOG injection, as is the case in the WT mouse.

We generated OIR in WT and HIF-1α KO mice, comparing DMOG-injected animals with PBS-injected controls, to determine whether hepatic HIF-1 is required for retinal protection in OIR. Lectin staining of retinal flat mounts and *in vivo* confocal scanning laser ophthalmoscopy with fluorescein angiography (Figure 3A) were used to quantify retinovascular ischemia, tortuosity, and neovascularization (Figure 3, B–D). A lack of response to DMOG in hepatic HIF-1α KO mice undergoing OIR was observed by persistent capillary dropout and tortuosity on retinal flat mounts, whereas significant reduction and elimination of these vascular pathologies was seen in DMOG-injected WT mice undergoing OIR (Figure 3A). These observations were quantified by automated vascular analysis, which showed that avascularity ($P < 0.0001$) and vascular tortuosity ($P < 0.01$) were decreased in DMOG-treated WT mice compared to PBS-treated WT mice, but that there was no difference in DMOG-treated versus PBS-treated HIF-1α KO mice (Figure 3, B–D).

We evaluated retinas from normoxic HIF-1α KO mice and compared them to control retinas from normoxic WT mice at P17 using toluidine blue-stained cross sections, lectin-stained flat mounts, and *in vivo* fluorescein angiography (Figure 4A) to determine whether loss of hepatic HIF-1α would impact normal retinal development. Compared to age-matched WT controls, superficial and deep vessels in the HIF-1α KO mice

appeared to be grossly normal at P17. Histopathological analysis of the liver, kidney, and brain also revealed normal architecture and cell appearance (Figure 4B).

## Biochemical Evidence of HIF Stabilization: DMOG-Mediated Activation of Liver HIF-1α Is Associated with Increasing EPO mRNA

Previous reports[32] demonstrated that EPO, an HIF-regulated cytokine with angioprotective action, lessened the effect of hyperoxia in mice. DMOG caused a rapid increase in serum EPO protein that was attenuated in the HIF-1α KO measured by ELISA (Figure 5A) and Western blot analysis (Figure 5, B and C). A comparison of the change in EPO mRNA from murine organs after 5 days of hyperoxia at P12 to the peak of hypoxic ischemia at P17 demonstrated both the tropism of DMOG for the liver and its ability to make the liver, normally unresponsive to environmental oxygen saturation, act as an endocrine organ after systemic hypoxia mimetic treatment with DMOG (Figure 5D). Both the kidney and eye responded to hypoxia by increasing EPO synthesis, whereas the liver showed no response to hyperoxia/hypoxia. Yet, it is the liver alone that has a significantly increased expression of EPO from i.p. DMOG. The increase in EPO mRNA peaks at 200-fold in the liver (Figure 5E), 6-fold in the kidney (Figure 5F), and 1.5-fold in the retina (Figure 5G), in synchrony with our previous findings[24] by Western blot analysis and luminometry indicating that liver PHD is the primary target of systemic DMOG.

## Cellular Evidence of HIF Stabilization: DMOG-Mediated Prevention of OIR Induces Bone-Marrow–Derived EPCs

HIF-regulated proteins are reported to regulate various cellular functions, including hematopoiesis, angiogenesis, cellular protection, DNA repair, and progenitor stem cell development.[33,34] In addition, several studies have demonstrated that EPO alone may induce bone-marrow–derived endothelial precursor cells that are recruited to the retina after systemic administration of exogenous EPO.[32,35] EPCs are bone-marrow–derived angiogenic cells (BMDACs) that have been identified based on double-positivity for the cell-surface receptors cKit and Sca1, as well as by more stringent criteria using triple-positivity for cKit, Sca1, and VEGFR2.[36–38] Using flow cytometry to identify double- and triple-positive cells, we observed a statistically significant increase in circulating bone-

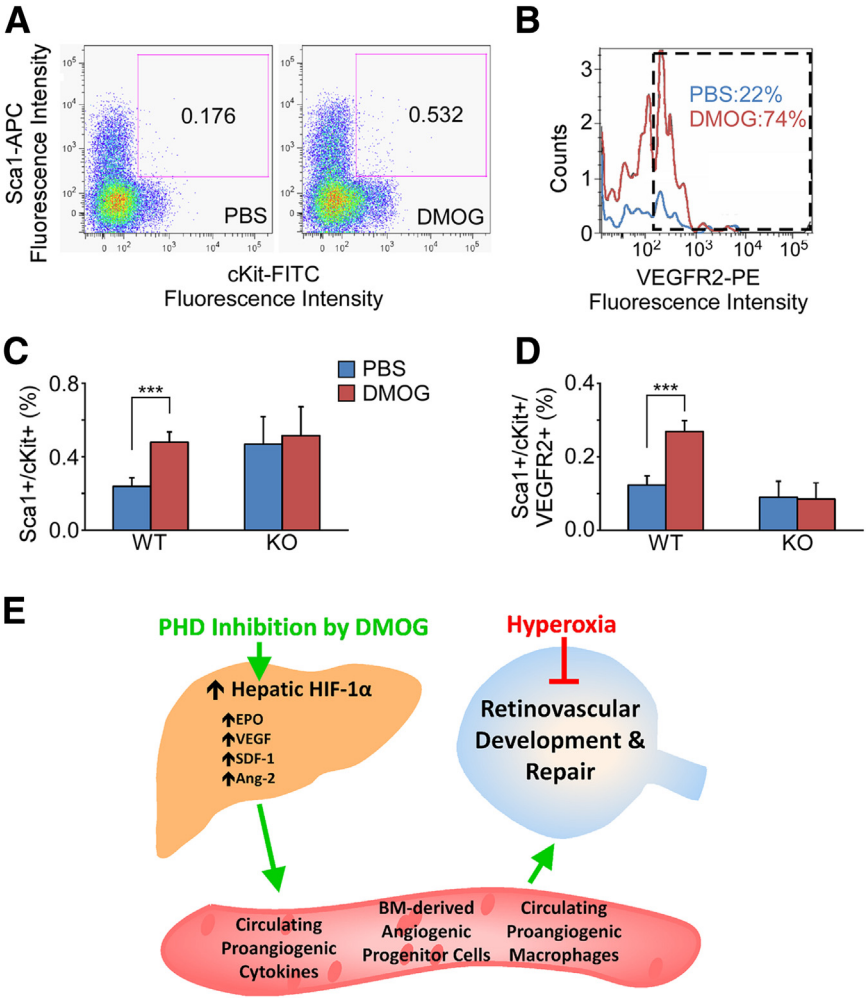


**Figure 6** An increase in circulating EPCs was seen in response to DMOG in WT mice but not in HIF-1α KO mice. Scatterplot of flow cytometry fluorescence intensity isolates percentages of peripheral blood leukocytes that were double-positive for Sca1/cKit (**A** and **C**) and the histogram of triple-positive for Sca1/cKit/VEGFR2 (**B** and **D**). There was a significant increase in circulating EPCs in response to DMOG in WT mice; however, there was no such response seen in the HIF-1α KO mice (***$P < 0.001$). **E:** Overall model of how the liver can be stimulated to act as an endocrine organ to protect distal capillary beds such as in the eye and specifically the retina. Data are expressed as means ± SEM (**C** and **D**). $n = 6$ mice per group (**C** and **D**). APC, allophyocyanin; FITC, fluorescein isothiocyanate; PE, phycoerythrin.

marrow−derived EPCs at 12 hours after treatment in WT mice injected with DMOG versus PBS controls (Figure 6, A and B). This increase in triple-positive, circulating EPCs was not present, however, when HIF-1α KO mice were injected with DMOG ($P = 0.001$) (Figure 6, C and D). The data presented here provide an HIF-1−dependent mechanism in which the liver could be induced to protect retinal blood vessels (Figure 6E).

## Discussion

The hypothesis of this investigation is that a visceral organ, such as the liver, could be stimulated to protect retinal capillary beds. We identified DMOG as a small molecule that inhibits HIF PHD in the liver, demonstrated both structural and functional protection against oxygen toxicity after systemic treatment with this small molecule, and then showed an absence of protection when *HIF1A* gene expression was ablated in the liver. Although it is natural to suspect that stabilizing an angiogenic activator of transcription during hyperoxia, a time when HIF is normally inactivated, is protective, these data develop the novel paradigm of a visceral organ initiating protection of a peripheral capillary bed. We speculate that the affinity of DMOG to a hepatic PHD may be related to dose, expression of and/or specificity for tissue-specific PHD isoforms in the neonatal mouse, or the half-life of DMOG. This may be a new arena for systems pharmacology, or the unification of systems biology and pharmacology, recently highlighted by the National Institute of General Medical Sciences of the NIH as a new field of study.[39] The evidence that we provide in this study suggests that the liver a good substrate to integrate systems biology and pharmacology to understand the complexity of drug action, in this case HIF stabilization, and to develop new insights into the systems biology of angiogenesis. Our HIF-1α KO can be used as a molecular platform to identify the role of liver-specific, secreted cytokines in protecting peripheral capillary beds.

Current concepts in HIF-mediated protective response to disease involve mobilization and subsequent homing of BMDACs.[40] For example, a combination approach to treating experimental limb ischemia is generated by first using tissue injection of an adenovirus encoding a constitutive form of HIF-1α (AdCA5), followed by transfer of BMDACs cultured in DMOG. The AdCA5 hypothetically generates a homing signal for BMDACs but is effective only if cells are pretreated with DMOG.[36] Our data suggest that inducing HIF-1 activity in a visceral organ might be capable of achieving both cytokine and cellular facets of the staged approach to peripheral vascular protection. A key point is that we intervened during the causative phase of ischemia, in this case hyperoxia, whereas most applications of proangiogenic, pro−HIF-1 strategies target tissues that are already ischemic. The latter approach may drive pathogenic angiogenesis in susceptible tissues that are already ischemic. Rescue of the protected phenotype of the HIF-1α KO by stimulating of BMDACs may provide direct support for the role of these cells in protecting retinal blood vessels.

The human counterpart of experimental OIR, ROP, is a leading cause of childhood blindness, annually blinding between 75,000 and 100,000 children worldwide. HIF PHDi might be one approach to preventing blindness in premature infants if it is administered early in postnatal life, thereby permitting life-saving oxygen therapy while inducing developing premature tissues to be resistant to oxygen toxicity. The fact that the liver is central to this protective response simplifies drug delivery because the liver is a first-pass organ, suggesting that intravenous or oral administration of suitable small-molecule inhibitors is an acceptable, potentially noninvasive approach to the treatment of ROP.

In summary, we demonstrate the feasibility of hypoxia mimetic treatment to target a visceral organ, liver, to prevent the disease phenotype in peripheral capillary beds, such as in the retina. The simplicity of targeting a central visceral organ through an HIF-1−dependent mechanism might justify angioprotection in diseases that need only a brief open window for therapy, such as ROP.

## Acknowledgments

We thank Amit Vasanji, Brent Bell, and Charles Kaul for imaging assistance; Gregory Grossman, Vera Bonhila, and Brian Rubin for histology preparation and analysis; Alecia Cutler and Kewal Assosingh for flow cytometry assistance; Rebecca Brown for technical assistance; and Bela Anand-Apte for suggestions during preparation of the manuscript.

## References

1. Hartnett ME, Penn JS: Mechanisms and management of retinopathy of prematurity. N Engl J Med 2012, 367:2515−2526
2. Steinkuller PG, Du L, Gilbert C, Foster A, Collins ML, Coats DK: Childhood blindness. J AAPOS 1999, 3:26−32
3. Park AM, Sanders TA, Maltepe E: Hypoxia-inducible factor (HIF) and HIF-stabilizing agents in neonatal care. Semin Fetal Neonatal Med 2010, 15:196−202
4. Ivan M, Kondo K, Yang H, Kim W, Valiando J, Ohh M, Salic A, Asara JM, Lane WS, Kaelin WG Jr: HIFalpha targeted for VHL-mediated destruction by proline hydroxylation: implications for O2 sensing. Science 2001, 292:464−468
5. Jaakkola P, Mole DR, Tian YM, Wilson MI, Gielbert J, Gaskell SJ, von Kriegsheim A, Hebestreit HF, Mukherji M, Schofield CJ, Maxwell PH, Pugh CW, Ratcliffe PJ: Targeting of HIF-alpha to the von Hippel-Lindau ubiquitylation complex by O2-regulated prolyl hydroxylation. Science 2001, 292:468−472
6. Yu F, White SB, Zhao Q, Lee FS: HIF-1alpha binding to VHL is regulated by stimulus-sensitive proline hydroxylation [erratum in: Proc Natl Acad Sci U S A 2001, 98:14744]. Proc Natl Acad Sci U S A 2001, 98:9630−9635
7. Masson N, Willam C, Maxwell PH, Pugh CW, Ratcliffe PJ: Independent function of two destruction domains in hypoxia-inducible factor-alpha chains activated by prolyl hydroxylation. EMBO J 2001, 20:5197−5206
8. Epstein AC, Gleadle JM, McNeill LA, Hewitson KS, O'Rourke J, Mole DR, Mukherji M, Metzen E, Wilson MI, Dhanda A, Tian YM,

Masson N, Hamilton DL, Jaakkola P, Barstead R, Hodgkin J, Maxwell PH, Pugh CW, Schofield CJ, Ratcliffe PJ: C. elegans EGL-9 and mammalian homologs define a family of dioxygenases that regulate HIF by prolyl hydroxylation. Cell 2001, 107:43–54
9. Bruick RK, McKnight SL: A conserved family of prolyl-4-hydroxylases that modify HIF. Science 2001, 294:1337–1340
10. Wang GL, Semenza GL: General involvement of hypoxia-inducible factor 1 in transcriptional response to hypoxia. Proc Natl Acad Sci U S A 1993, 90:4304–4308
11. Jiang BH, Rue E, Wang GL, Roe R, Semenza GL: Dimerization, DNA binding, and transactivation properties of hypoxia-inducible factor 1. J Biol Chem 1996, 271:17771–17778
12. Semenza GL: Hypoxia-inducible factor 1: master regulator of O2 homeostasis. Curr Opin Genet Dev 1998, 8:588–594
13. Semenza GL, Wang GL: A nuclear factor induced by hypoxia via de novo protein synthesis binds to the human erythropoietin gene enhancer at a site required for transcriptional activation. Mol Cell Biol 1992, 12:5447–5454
14. Manalo DJ, Rowan A, Lavoie T, Natarajan L, Kelly BD, Ye SQ, Garcia JG, Semenza GL: Transcriptional regulation of vascular endothelial cell responses to hypoxia by HIF-1. Blood 2005, 105:659–669
15. Pierce EA, Foley ED, Smith LE: Regulation of vascular endothelial growth factor by oxygen in a model of retinopathy of prematurity. Arch Ophthalmol 1996, 114:1219–1228
16. Alon T, Hemo I, Itin A, Pe'er J, Stone J, Keshet E: Vascular endothelial growth factor acts as a survival factor for newly formed retinal vessels and has implications for retinopathy of prematurity. Nat Med 1995, 1:1024–1028
17. Claiborn K: William G. Kaelin Jr. and Gregg L. Semenza receive the 2012 ASCI/Stanley J. Korsmeyer Award. J Clin Invest 2012, 122:1136–1137
18. Rankin EB, Biju MP, Liu Q, Unger TL, Rha J, Johnson RS, Simon MC, Keith B, Haase VH: Hypoxia-inducible factor-2 (HIF-2) regulates hepatic erythropoietin in vivo. J Clin Invest 2007, 117:1068–1077
19. Ratan RR, Siddiq A, Aminova L, Langley B, McConoughey S, Karpisheva K, Lee HH, Carmichael T, Kornblum H, Coppola G, Geschwind DH, Hoke A, Smirnova N, Rink C, Roy S, Sen C, Beattie MS, Hart RP, Grumet M, Sun D, Freeman RS, Semenza GL, Gazaryan I: Small molecule activation of adaptive gene expression: tilorone or its analogs are novel potent activators of hypoxia inducible factor-1 that provide prophylaxis against stroke and spinal cord injury. Ann N Y Acad Sci 2008, 1147:383–394
20. Siddiq A, Aminova LR, Troy CM, Suh K, Messer Z, Semenza GL, Ratan RR: Selective inhibition of hypoxia-inducible factor (HIF) prolyl-hydroxylase 1 mediates neuroprotection against normoxic oxidative death via HIF- and CREB-independent pathways. J Neurosci 2009, 29:8828–8838
21. Eckle T, Köhler D, Lehmann R, El Kasmi K, Eltzschig HK: Hypoxia-inducible factor-1 is central to cardioprotection: a new paradigm for ischemic preconditioning. Circulation 2008, 118:166–175
22. Willam C, Maxwell PH, Nichols L, Lygate C, Tian YM, Bernhardt W, Wiesener M, Ratcliffe PJ, Eckardt KU, Pugh CW: HIF prolyl hydroxylases in the rat; organ distribution and changes in expression following hypoxia and coronary artery ligation. J Mol Cell Cardiol 2006, 41:68–77
23. Sarkar K, Fox-Talbot K, Steenbergen C, Bosch-Marcé M, Semenza GL: Adenoviral transfer of HIF-1alpha enhances vascular responses to critical limb ischemia in diabetic mice [erratum in: Proc Natl Acad Sci U S A 2010;107:513]. Proc Natl Acad Sci U S A 2009, 106:18769–18774
24. Sears JE, Hoppe G, Ebrahem Q, Anand-Apte B: Prolyl hydroxylase inhibition during hyperoxia prevents oxygen-induced retinopathy. Proc Natl Acad Sci U S A 2008, 105:19898–19903
25. Huang H, Van de Veire S, Dalal M, Parlier R, Semba RD, Carmeliet P, Vinores SA: Reduced retinal neovascularization, vascular permeability, and apoptosis in ischemic retinopathy in the absence of prolyl hydroxylase-1 due to the prevention of hyperoxia-induced vascular obliteration. Invest Ophthalmol Vis Sci 2011, 52:7565–7573
26. Duan LJ, Takeda K, Fong GH: Prolyl hydroxylase domain protein 2 (PHD2) mediates oxygen-induced retinopathy in neonatal mice. Am J Pathol 2011, 178:1881–1890
27. Trichonas G, Lee TJ, Hoppe G, Au J, Sears JE: Prolyl hydroxylase inhibition during hyperoxia prevents oxygen-induced retinopathy in the rat 50/10 model. Invest Ophthalmol Vis Sci 2013, 54:4919–4926
28. Safran M, Kim WY, O'Connell F, Flippin L, Günzler V, Horner JW, Depinho RA, Kaelin WG Jr: Mouse model for noninvasive imaging of HIF prolyl hydroxylase activity: assessment of an oral agent that stimulates erythropoietin production. Proc Natl Acad Sci U S A 2006, 103:105–110
29. Smith LE, Wesolowski E, McLellan A, Kostyk SK, D'Amato R, Sullivan R, D'Amore PA: Oxygen-induced retinopathy in the mouse. Invest Ophthalmol Vis Sci 1994, 35:101–111
30. Connor KM, Krah NM, Dennison RJ, Aderman CM, Chen J, Guerin KI, Sapieha P, Stahl A, Willett KL, Smith LE: Quantification of oxygen-induced retinopathy in the mouse: a model of vessel loss, vessel regrowth and pathological angiogenesis. Nat Protoc 2009, 4:1565–1573
31. Stahl A, Connor KM, Sapieha P, Willett KL, Krah NM, Dennison RJ, Chen J, Guerin KI, Smith LE: Computer-aided quantification of retinal neovascularization. Angiogenesis 2009, 12:297–301
32. Chen J, Connor KM, Aderman CM, Smith LE: Erythropoietin deficiency decreases vascular stability in mice. J Clin Invest 2008, 118:526–533
33. Arcasoy MO: The non-haematopoietic biological effects of erythropoietin. Br J Haematol 2008, 141:14–31
34. Bahlmann FH, De Groot K, Spandau JM, Landry AL, Hertel B, Duckert T, Boehm SM, Menne J, Haller H, Fliser D: Erythropoietin regulates endothelial progenitor cells. Blood 2004, 103:921–926
35. Smith LE: Through the eyes of a child: understanding retinopathy through ROP the Friedenwald lecture. Invest Ophthalmol Vis Sci 2008, 49:5177–5182
36. Rey S, Lee K, Wang CJ, Gupta K, Chen S, McMillan A, Bhise N, Levchenko A, Semenza GL: Synergistic effect of HIF-1alpha gene therapy and HIF-1-activated bone marrow-derived angiogenic cells in a mouse model of limb ischemia. Proc Natl Acad Sci U S A 2009, 106:20399–20404
37. Jujo K, Hamada H, Iwakura A, Thorne T, Sekiguchi H, Clarke T, Ito A, Misener S, Tanaka T, Klyachko E, Kobayashi K, Tongers J, Roncalli J, Tsurumi Y, Hagiwara N, Losordo DW: CXCR4 blockade augments bone marrow progenitor cell recruitment to the neovasculature and reduces mortality after myocardial infarction. Proc Natl Acad Sci U S A 2010, 107:11008–11013
38. Chanda D, Kumar S, Ponnazhagan S: Therapeutic potential of adult bone marrow-derived mesenchymal stem cells in diseases of the skeleton. J Cell Biochem 2010, 111:249–257
39. Rogers M, Lyster P, Okita R: NIH Support for the Emergence of Quantitative and Systems Pharmacology. CPT Pharmacometrics Syst Pharmacol 2013, 2:e37
40. Semenza GL: Hypoxia-inducible factors in physiology and medicine. Cell 2012, 148:399–408